nanomanufacturing

MDPI

Article

Safe Explosion Works Promoted by 2D Graphene Structures Produced under the Condition of Self-Propagation High-Temperature Synthesis

Alexander Petrovich Voznyakovskii [1,*], Mikhail Alekseevich Ilyushin [2], Aleksei Alexandrovich Vozniakovskii [3], Irina Vladimirovna Shugalei [2] and Georgy Georgievich Savenkov [2,3]

[1] Lebedev Research Institute for Synthetic Rubber, 198035 Saint Petersburg, Russia
[2] St. Petersburg State Institute of Technology, 190013 Saint Petersburg, Russia; explaser1945@gmail.com (M.A.I.); shugalei@mail.ru (I.V.S.); sav-georgij@yandex.ru (G.G.S.)
[3] Ioffe Institute, 194021 Saint Petersburg, Russia; alexey_inform@mail.ru
* Correspondence: voznap@mail.ru

Abstract: The paper presents the results of a study on the effectiveness of few-layer graphene synthesized under SHS conditions from lignin as a modifying additive in creating composite pyrotechnic complexes based on porous silicon and calcium perchlorate. It was found that the addition of few-layer graphene (20–30 wt. %) could significantly increase the probability of the ignition of pyrotechnic compositions by laser diode (infrared) radiation (wavelength of 976 nm and power of 15 MW/m^2) compared to the initial pyrotechnic compositions. Using few-layer graphene also leads to a sharp increase in sensitivity to infrared laser radiation and the initiation of explosive transformations in retrofitted pyrotechnic compositions compared to the initial pyrotechnic compositions. Due to the high productivity and low cost of the technique for synthesizing few-layer graphene, the use of composite pyrotechnic compositions modified with few-layer graphene is profitable in the actual industry. A phenomenological model of the formation mechanism of 2D graphene structures under the conditions of the SHS process is proposed.

Keywords: self-propagating high-temperature synthesis; few-layer graphene; laser initiation; pyrotechnic composition

Citation: Voznyakovskii, A.P.; Ilyushin, M.A.; Vozniakovskii, A.A.; Shugalei, I.V.; Savenkov, G.G. Safe Explosion Works Promoted by 2D Graphene Structures Produced under the Condition of Self-Propagation High-Temperature Synthesis. *Nanomanufacturing* **2024**, *4*, 45–57. https://doi.org/10.3390/nanomanufacturing4010003

Academic Editor: Asterios (Stergios) Pispas

Received: 9 November 2023
Revised: 23 December 2023
Accepted: 4 February 2024
Published: 8 February 2024

1. Introduction

The high-energy pulsed impact of explosive decomposition products of energetic materials (EMs) on different environmental objects is the basis of many modern industrial technologies. In this regard, creating new technologies related to the controlled impact of a pulsed action on materials is an essential promising direction in mining, metallurgical engineering, oil-extracting industries, construction, and mechanical engineering.

These methods can be used for the explosive cutting of reinforced concrete structures, crushing and loosening of rocks, special processing of slabs and nonmetallic materials, cleaning surfaces, containers, and holes from ice and metal, and compacting hard-to-press powders [1].

In practice, the safe use of energy materials (EMs) cannot be guaranteed due to aging processes during long-term storage. Thus, it is impossible to eliminate the risk of the unpredictable explosive decomposition of EMs due to the influence of random external factors [2].

The transition from electrical means of initiation to laser ones is a promising solution to these problems. So, using laser detonators eliminates the need to connect electrical wires to the initiation means, making the laser detonators (LDs) immune to threats, such as electrostatic discharge, stray currents, or lightning.

Using fiber optic communication lines between the laser source and the LDs also increases the safety of blasting compared to traditional electrical blasting methods [3].

Another significant advantage of LDs is the possibility of replacing toxic, highly sensitive to mechanical impacts primary explosives in the blasting means with less toxic and less sensitive EMs, for example, photosensitive pyrotechnic compositions [4]. It has presently become clear that the effectiveness of laser detonators can be significantly improved when nanocarbon is introduced into their assembly [5]. At the same time, graphene is increasingly used as a nanocarbon component of the EMs (for example, work [6] and the references therein).

The choice of graphene is currently associated with its ability to form a flow of electrons under the influence of an external photon stream [7]. Accordingly, the use of graphene as a component of the laser devices can provide a synergistic effect of the influence of the thermal energy flow and the laser photon stream of the EMs [8–10].

However, despite the demonstrated high efficiency of graphene's use in the laser detonator's design, such detonators are still not used in actual pyrotechnic products. This is because the performance of even the most productive methods of graphene structure synthesis is insufficient for the tasks of modern materials science and, in particular, for the rapidly developing blasting technologies. It should also be noted that modern, stringent environmental requirements are an essential factor for determining the prospects for scaling up known and newly developed graphene synthesis methods. Therefore, many research groups constantly seek new possibilities for synthesizing graphene-like structures, meeting these challenges.

When developing graphene advanced synthesis methods, researchers have to choose between techniques producing classical graphene that are impossible to provide the required level of performance and more productive techniques that lead to 2D graphene structures, meeting the requirements of a specific task such as laser detonator creation.

Previously, we proposed a method for synthesizing 2D graphene structures by carbonizing biopolymers under a self-propagating high-temperature synthesis (SHS) conditions that meets the requirements presented above [11].

The term SHS refers to moving a spin wave of a solid exothermic reaction through a mixture of reagents (oxidizing agent and reducing agent), where the heat release is located in the thin layer and is transferred from layer to layer by heat transfer [12]. In the SHS process, branched-chain ignition, in contrast to thermal ignition, is caused by an avalanche multiplication of active intermediate products—free atoms, radicals, and excited particles—in their rapid reactions with the initial reagents and among themselves [13]. The advantages of SHS methods are the high synthesis rates, the possibility of carrying out the process without a constant supply of energy from external power sources, the possibility of synthesizing in any atmosphere or vacuum, and the absence of fundamental scale restrictions [14,15]. It should be noted that the synthesis of 2D nanocarbons under the conditions of the SHS process proceeds according to the "bottom-up" mechanism [16].

The stages of the "bottom-up" mechanism include successive processes of the thermolysis of the biopolymer to some primitives and the processes of their self-organization into 2D structures.

However, the 2D nanocarbons (Gsvs) obtained in the SHS process do not correspond in their morphometric parameters to the graphene samples obtained using known methods, so this does not allow us to recommend this method as an alternative to EM charges.

The purpose of this work is to develop a new method of complete 2D graphene structure synthesis and demonstrate the possibility of its application as a component of initiating energetic compositions with low laser ignition thresholds.

2. Experimental Part

2.1. Materials

Precursor

Lignin, a complex, irregularly structured, resistant to decomposition, insoluble in water and organic solvents, high-molecular-weight polymer with branched macromolecules of a cyclic structure, was used as a precursor [17]. The lignin used in the experiments was obtained from long-term storage dumps from the Arkhangelsk hydrolysis plant under atmospheric conditions.

The choice of lignin as a precursor of graphene-like material is explained by its reserves accumulated at storage sites in millions of tons, which poses a severe environmental threat [18]. In this regard, the choice of lignin as a precursor to graphene structures was also due to the desire to develop a method for its utilization to have some benefit.

2.2. Synthesis of Few-Layer Graphene (FLG)

The synthesis of 2D graphene structures was carried out by carbonizing lignin under the self-propagating high-temperature synthesis process (Figure 1) [11].

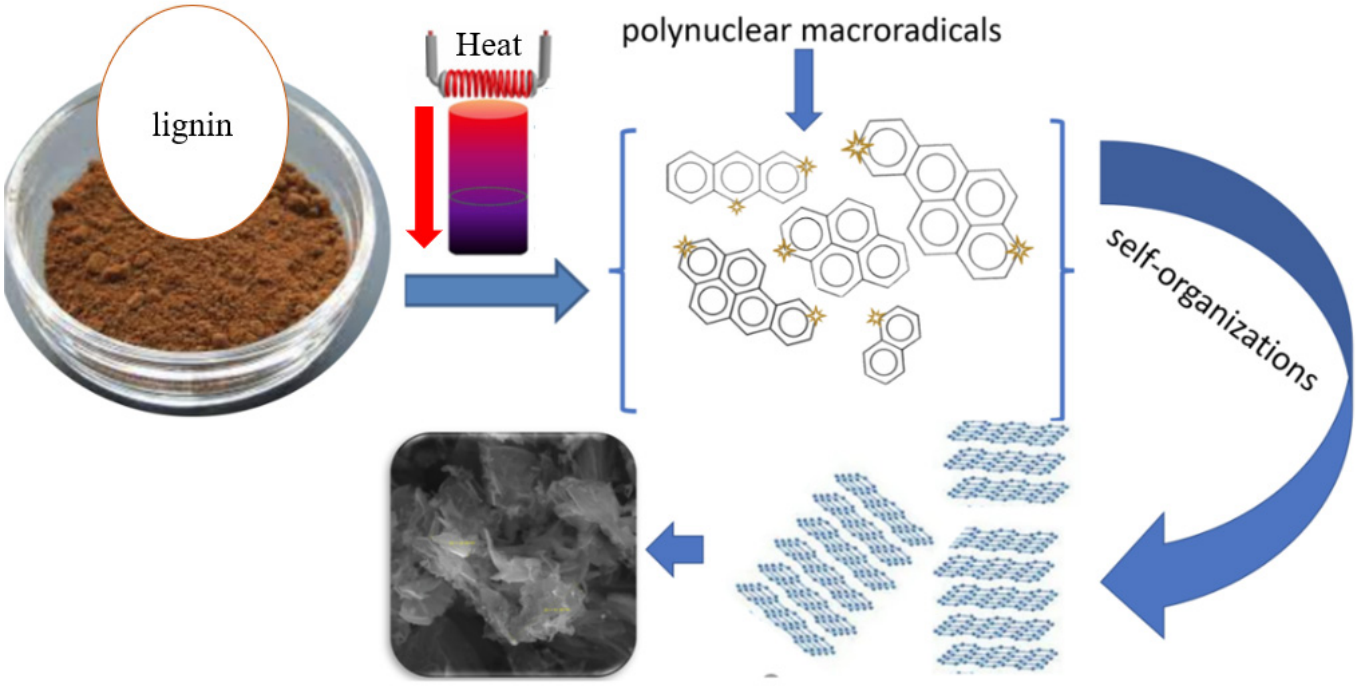

Figure 1. Diagram of graphene structures' synthesis by lignin carbonization under the conditions of the process of self-propagating high-temperature synthesis.

The method of obtaining FLG was carried out using a laboratory reactor, which is a quartz vessel (capacity 1 l) with a heating element in the lower part, which provides the initial heating of the reaction zone to the temperature required to initiate the process (220 °C).

The temperature in the reaction zone was controlled using a thermocouple. The preparation of the synthesis included several successive stages. The pre-dried lignin was transferred to a ball mill and grounded for 15 min.

Next, a mechanical mixture of an oxidizing agent (ammonium nitrate NH_4NO_3, chemically pure, Sigma-Aldrich, St. Louis, MI, USA) and a precursor (lignin) was prepared in a 1:1 weight ratio. The prepared mechanical mixture of the oxidizer and precursor was placed in a "drunk barrel"-type mixer and stirred for 15 min.

Then, the resulting crushed mixture was transferred to a reactor preheated and purged with a current of dry argon. The start and end of the reaction were recorded by the

beginning and end of the release of gaseous reaction products. The duration of the process was equal to 5–8 min. The yield of the carbonization product (based on the precursor) was 30–35% wt. The rest of the reaction mass passed into the gas phase and was captured in a trap cooled with liquid nitrogen.

2.3. Methods Used for Studying the Resulting Carbonized Structures

2.3.1. XRD Diffraction

The phase composition of the synthesized samples was studied using diffraction patterns recorded on an XRD-7000 diffractometer (CuKα radiation, λ = 0.154051 nm) (Shimadzu, Kyoto, Japan).

2.3.2. Raman Spectroscopy

The quality of the synthesized samples was estimated using Raman spectra recorded on a Horiba Jobin Yvon LabRam HR 800 spectrometer (532 nm laser; 1800 g/mm diffraction grating; micro-Raman system, microscopic objective, and optical magnification $\times$20), Horiba, Tokyo, Japan.

2.3.3. SEM and TEM

The images of FLG were obtained by scanning electron microscopy on a TESCAN Mira-3M microscope (TESCAN, Brno, Czech Republic) with an Oxford Instruments X-max EDX accessory (Oxford Instruments, Abingdon, UK) and by transmission electron microscopy on a 50 kV FEI Tecnai G2 30 S-TWIN microscope. In the TEM study, the powder samples were placed in ethanol, sonicated for 5 min, and mounted on a carbon grid. The obtained ring XRD patterns were identified using the software implemented in the Rigaku Ultima-IV diffractometer.

2.3.4. Specific Surface Area Determination

The specific surface area of the synthesized samples was determined by polymolecular adsorption (BET method) using an ASAP 2020 Accelerated Surface Area and Porosimeter analyzer (Norcross, GA, USA). Nitrogen was used as an adsorbate gas. Prior to the measurements, heating in a vacuum at a temperature of 300 °C for 3 h was used as a standard sample preparation method. The measurement error was no more than 3%. The true density of FLG powder particles was determined by a helium pycnometer using an Ultrapycnometer 1000 device (Quantachrome Instruments, Boynton Beach, FL, USA).

2.4. Production of Pyrotechnic Compositions

A promising composition based on porous silicon was used as the base pyrotechnic composition [19], according to the method described in the article [20]. Nanoporous silicon (por-Si) with a porosity of 70–80% and an average pore size of 12–15 nm was obtained. In this work, we used nanoporous silicon powder with a 30–40 μm particle size.

2.4.1. Samples of Charge of the Pyrotechnic Composition (PC) Based on por-Si Powder and Calcium Perchlorate $Ca(ClO4)_2$

Samples of a pyrotechnic composition (PC) based on por-Si and calcium perchlorate $Ca(ClO_4)_2$ were prepared as follows: 18 mg of por-Si powder was pressed under a pressure of 80 MPa into a metal cap 4 mm high with an internal diameter of 4 mm and a hole in the bottom 3 mm in diameter. The pressed por-Si powder was impregnated with a solution of $Ca(ClO_4)_2$ in methanol so that, after the evaporation of the methanol, the mass ratio between $Ca(ClO_4)_2$ and por-Si powder was at the level of 1:1. The height of the PC charge in the cap was 3 mm. The caps with the charge of the resulting PC were dried in air and then dried in a thermostat at a temperature of 80 °C for 15 min until the solvent residues completely evaporated, which was controlled by weighing the caps (their mass became constant). The finished PC samples were tested for sensitivity to laser diode radiation.

2.4.2. Basic Composition Modified with Graphene Particle Preparations

To obtain samples of compositions PC-1 and PC-2, por-Si and FLG powder particles were mixed at a ratio between components (por-Si:FLG graphene) of 1:0.5 or 1:1 until a uniform color was obtained. Then, test samples were made from the resulting pyrotechnic compositions: a mixture (18 mg) was pressed into caps under a pressure of 80 MPa. The pressed powder of the mixture was impregnated with a solution of $Ca(ClO_4)_2$ in methanol so that, after the evaporation of methanol, the mass ratio between $Ca(ClO_4)_2$ and por-Si powder was at the level of 1:1. The caps with the charge of the resulting PC were dried in air and then dried in a thermostat at a temperature of 80 °C for 15 min until the solvent residues completely evaporated, which was controlled by weighing the caps (their mass became constant). Thus, the following PCs were obtained with the ratio between components (por-Si:$Ca(ClO_4)_2$:FLG graphene) 1:1:1 (PC-1) or 1:1:0.5 (PC-2). The PC-1 and PC-2 samples were tested for sensitivity to laser diode radiation.

2.4.3. Testing of Pyrotechnic Compositions

The susceptibility of PCs to laser radiation was studied with the help of a semiconductor laser diode of the Focuslight ECSE01-08-976 type (San Francisco, CA, USA) with a wavelength of 976 nm (infrared radiation) and an output power of up to 8 W. Under test conditions, PC charges were exposed to laser radiation with constant flux $q \approx 15$ MW/m^2. A Tektronix TDS2014 oscilloscope was used to record the burning time of a pressed PC placed in metal caps.

The oscilloscope detected the first signal at the moment the pulse was applied to the Focuslight FLFCSE01-8-976 laser diode, and the oscilloscope from the FD-256photosensor fixed the second signal at the moment the combustion front reached the free surface of the composition. The primary camera of an Honor 10 smartphone (16 MP, aperture f/1.8), frame rate of 720 fps (or 480 fps), recorded the process of PC burning after the laser ignition.

3. Results and Their Discussion

The lignin carbonization product turned out to be a highly dispersed black powder. Complementary research methods, such as electron microscopy, Raman spectroscopy, and X-ray diffraction, were used to confirm the stated model ideas for the carbonized product to have a graphene-like structure.

3.1. Electron Microscopy

Electron micrographs of the carbonized lignin are presented in Figure 2. From Figure 2, it can be concluded that the resulting particles have a volumetric–planar "scaly" form. These particles are typical for 2D carbon structures; see, for example [21,22].

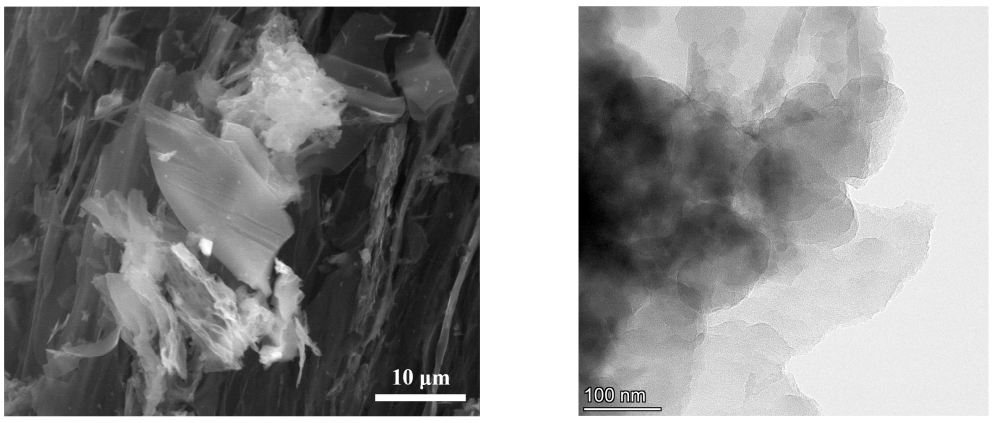

Figure 2. Electron micrographs of carbonized lignin: (**a**)—scanning electron microscopy (SEM); (**b**)—transmission electron microscopy (TEM) method.

Attention should be paid to the electron microscopy method as the most visual way to determine the morphology of the resulting carbonized product.

Spectroscopic studies should confirm the fine structure of the product. Spectroscopic studies were carried out to clarify the nature of the obtained product.

3.1.1. X-ray

The diffraction pattern of the carbonized product is shown in Figure 3. A narrow, intense peak can be observed in the diffraction patterns of graphite at 26.50. A weak, diffuse peak is typical for 2D carbon structures. The blurring of the XRD peak indicates that the particles are formed by a stack of several graphene sheets [23].

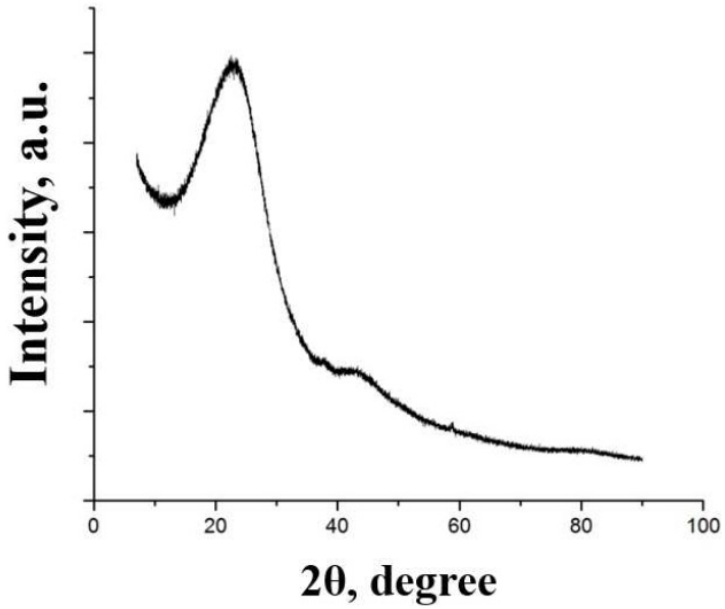

Figure 3. X-ray diffraction pattern of carbonized lignin obtained by self-propagating high-temperature synthesis.

3.1.2. Raman Spectroscopy

Raman spectroscopy is currently an effective way to determine the number of layers of 2D graphene structures without destroying their crystal lattice. In addition, the shape and position of the 2D peak all-overs clearly distinguish single-layer, bilayer, and multilayer graphene.

Single-layer graphene usually exhibits a single and sharp 2D peak below 2700 cm^{-1}, while bilayer graphene exhibits a broader and elevated 2D peak at 2700 cm^{-1}. In the case of graphene sheets with more than five layers, we see broad 2D peaks that are shifted to positions 2700 + (20 ÷ 40) cm^{-1} and are similar to the 2D peaks of bulk graphite.

Raman spectroscopy data are shown in Figure 4. The Raman spectrum has two distinct peaks—at 1300 cm^{-1} and 1590 cm^{-1}. The first peak reflects defects in the sp^2 lattice (peak D) and the other corresponds to hybridized carbon sp^2 (peak G). The relationship between D and G is the characteristics of each specific graphene structure sample, determined by the nature of the precursor and the synthesis method.

The true particle density of the carbonated product was observed. Additionally, such an essential characteristic of the carbonated product as its true density was determined. The measured value of the true density of the powder particles was equal to $\rho = 1.98 \pm 0.02$ g/cm^3. It coincided with the literature data for the true density of low-defect particles of few-layered graphene ($\rho = 2.21$ g/cm^3) [24].

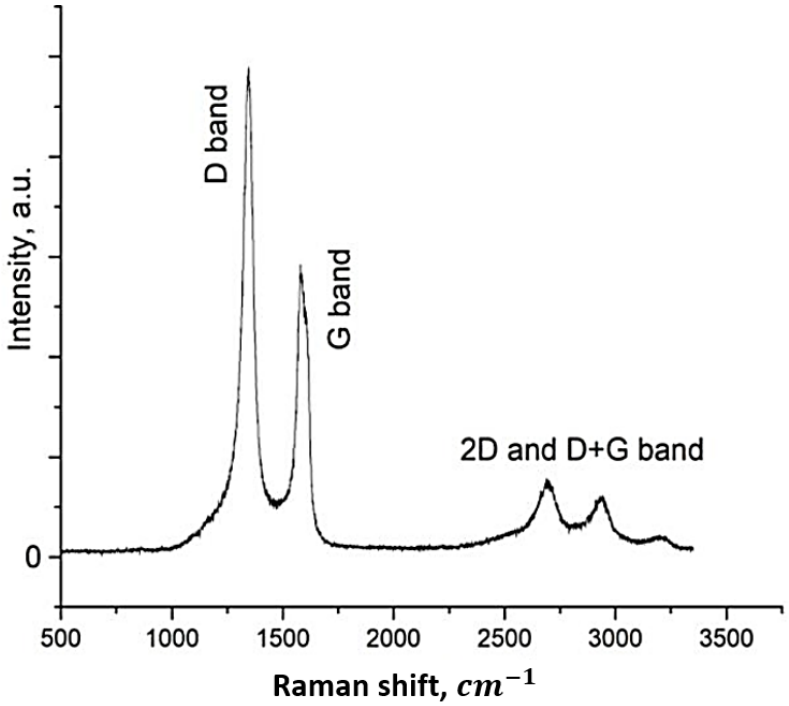

Figure 4. Raman scattering spectra for carbonized lignin particles (laser wavelength: 532 nm).

Summarizing the data of complementary electron microscopy methods and spectrometric analysis methods, namely the presence of a wide diffuse maximum around the value of 2θ = 26.5° in the diffraction pattern and the presence of three characteristic lines (peaks) in the Raman scattering spectrum of carbonized lignin samples, as well as the data for the true density allowed us to compare the obtained carbonized samples with the few-layer graphene samples described in literature [25–27]. Taking into account this method, we denoted it as FLGsvs.

4. Application of 2D Graphene Structures to Reduce the Ignition Threshold of Pyrotechnic Compositions

A pyrotechnic composition based on porous silicon and calcium perchlorate can likely replace traditional primary explosives (for example, lead azide) [28]. The advantage of this composition over traditional primary Ems is the absence of heavy and toxic metals in the composition. Previously, similar pyrotechnic compositions showed pretty high sensitivity to various electrophysical pulses (such as a high-current electron beam of nanosecond duration, a high-voltage discharge, and an electrical explosion of a semiconductor bridge) [29] and thermal effects [30]. However, their susceptibility to coherent radiation remained unexplored.

We started the work by studying the fundamental possibility of using PS in lasers as a means of ignition and initiation. At first, the susceptibility to radiation of a laser diode of a two-component pyrotechnic composition based on nanopore-Si powder and calcium perchlorate $Ca(ClO_4)_2$ was studied. During the experiment, five tests were carried out. In all cases, no ignition of charges was observed. It is known that graphene and its derivatives sensitize the Ems of various natures to coherent radiation. For example, when multilayer graphene was added, the threshold for ignition of a high-energy cobalt salt by a laser diode beam sharply decreased [31]. The work [32] proposed the use of graphene as a promising alloying component of solid rocket powders and primary and secondary explosives. The use of multilayer graphene as a promising alloying component of photosensitive PC based on fluorine rubber was demonstrated in [33]. Based on the presented data, we started to study the PC por-Si + $Ca(ClO_4)_2$ sensitivity sensitized with graphene FLGsvs to infrared radiation of a laser diode.

Two types of charges were prepared (see experimental part). Three charges of each type were examined while testing the samples; an explosive transformation (ignition with a solid sound effect) was observed in all six cases. This effect can be interpreted as explosive combustion. The sequence of processes of the explosive transformations of PC-1 and PC-2 charges are shown in Figures 5 and 6, respectively.

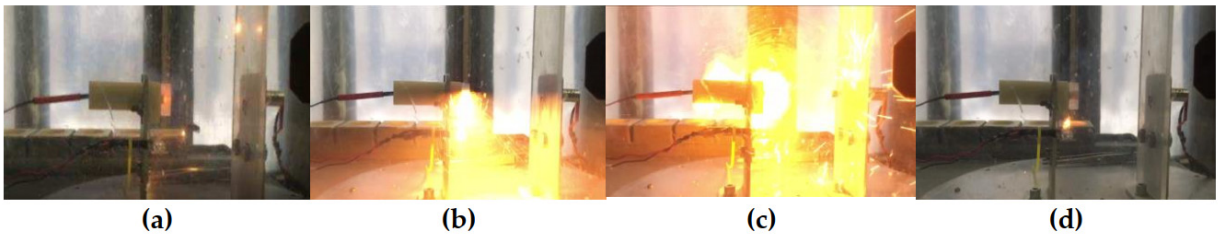

Figure 5. The process of the explosive transformation of the PC-1 charge: (**a**) the beginning of the combustion reaction; (**b**,**c**) formation of a large combustion area; (**d**) sample burnout.

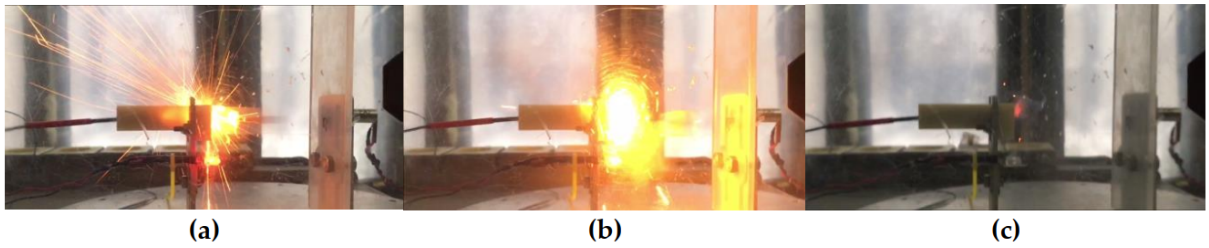

Figure 6. The burning sequence of the PC-2 charge: (**a**,**b**) formation of a large combustion area; (**c**) burnout of the charge.

The oscillograms of the deflagration of compositions PC-1 and PC-2 showed that their combustion rates differ. So, under experimental conditions, the PC-1 composition burnt out in ~10 ms (Figure 7a) and the PC-2 composition burnt faster in ~750 μs (Figure 7b).

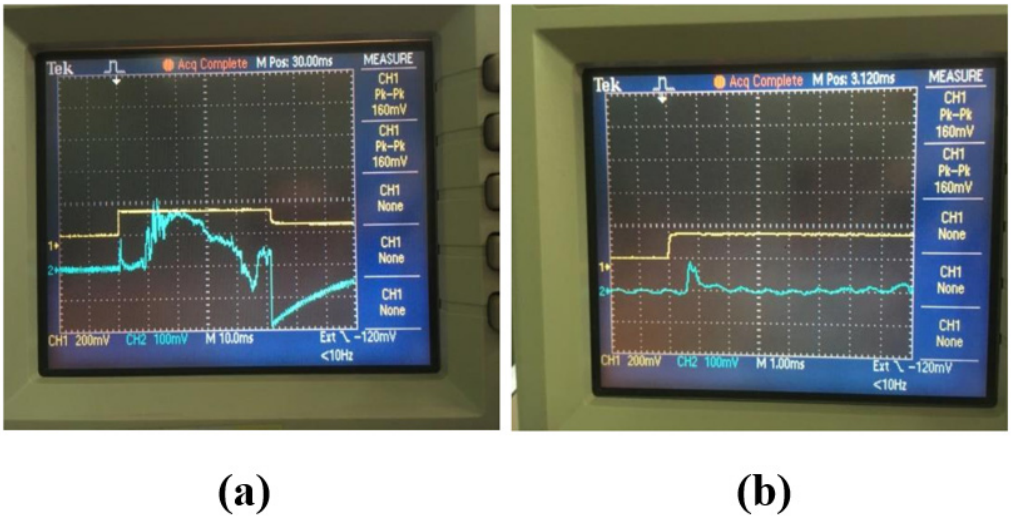

Figure 7. Oscillograms of tests on the burning rates of charges PC-1 (**a**) and PC-2 (**b**).

Thus, adding graphene-like material powder to pressed samples of PC-1 and PC-2 increased the likelihood of their ignition by laser diode (infrared) radiation compared with the original PC. Consequently, the addition of graphene-like powder FLGsvs increased the ignition ability of PC based on nanoporous silicon to laser diode (infrared) radiation. Moreover, if in the case of classical explosive compositions initiated with a laser beam, the share of the absorbing additive did not exceed (3–5)% (mass) (the amount of the sensitizing

additive over 5% (mass) resulted in failures during the laser excitations), in the case of the PC, the share of the sensitizing additive of FLGsvs could be (20–33)% (mass).

Since graphene nanostructures have record thermal conductivity values (up to 5000 W/(m × K) [34], their use as a modifying additive in the creation of composites [35] and nanofluids [36,37] can significantly increase the thermal conductivity of the original matrix. It can be assumed that, by using FLG, we increased the thermal conductivity of samples PC-1 and PC-2 compared to the unmodified sample. If our assumption is correct, then due to higher thermal conductivity, the energy from the laser is much better transferred throughout the sample volume, which leads to a sharp increase in sensitivity to infrared laser radiation and the excitation of explosive transformations in the PC.

5. Model Representations of the Mechanism of Formation of 2D Graphene Structures under the Condition of the SHS Process

Analyzing the experimental results, we tried to provide some considerations of the mechanism of carbonization of organic compounds with the formation of all nootropic forms of nanocarbon. As can be observed from the analysis of the literature, the first real example of obtaining an allotropic form of nanocarbon by the carbonization of organic molecules is the synthesis of 3D nanocarbon (detonation nanodiamonds: DNDs) as the result of the explosive decomposition of the mixture of two organic molecules—trinitrotoluene and cyclotrimethylenetrinitramine (RDX) [38]. The most straightforward idea of the mechanism of the carbonization of organic compounds in the process of detonation synthesis is the idea of their carbonization mechanism being achieved through breaking the covalent bonds of the atoms of the original molecules up to their complete atomization [39]. However, the activation energy of such reactions is very high and cannot be provided under the conditions of the detonation synthesis process [40]. Consequently, even under conditions of high pressure and temperature during the explosive decomposition of trinitrotoluene and cyclotrimethylenetrinitramine, the destruction of their molecules only applies to some primitive, carbon structures, which, in subsequent self-organization processes, form 3D nanocarbon particles (DNDs). Several studies have shown that the specific morphometric parameters of DND particles depend on the conditions of detonation synthesis and the nature of the precursor (original explosive) [41]. It should be noted that, despite the large number of works, the reliable structure of the resulting primitives is unknown and, to date, has been based only on phenomenological models.

Creating a model for the formation of allotropic forms of nanocarbon within the framework of the carbonization mechanism of organic molecules, we should proceed from the model developed by N.N. Semenov [42]. According to this theory, the probable mechanism of the destruction of materials is the mechanism associated with forming chemical radicals that, in turn, include multiple successive shear movements of atoms. Thus, covalent bond breaking is not a result, but a consequence of the synergistic effect of elementary acts with lower activation energy. As a result, the energy of covalent bond breaking is reduced, leading to their breaking. In terms of such a model of material destruction, one can assume that the amount of energy supplied to the system plays a crucial role in determining the structure of final nanocarbons during the carbonization of organic substances.

To test the proposed model, we carried out a detonation synthesis under conditions corresponding to the production of DNDs [43] but excluding hexogen from the charge composition, using only trinitrotoluene as a nanocarbon precursor. The exclusion of hexogen from the composition of the charge reduced the energy of its explosive decomposition [44]. To characterize the carbonized product synthesized under conditions of energy-deficient detonation synthesis, we used a set of complementary research methods already used in the work.

A comparison of the data in Figures 2 and 4 with the data in Figures 8 and 9 allowed us to conclude that energy-deficient detonation synthesis did not lead to the formation of 3D nanocarbon, but resulted in the formation of 2D graphene structures. It should be noted

that, although both SHS synthesis and energy-deficient detonation synthesis led to the formation of 2D graphene structures, the particles of the synthesized nanocarbons differed in their morphometric parameters. A rigorous comparison of the morphometric parameters of the synthesized particles with the help of different methods from various precursors of 2D graphene structures lies beyond the scope of this work and will be analyzed in future publications.

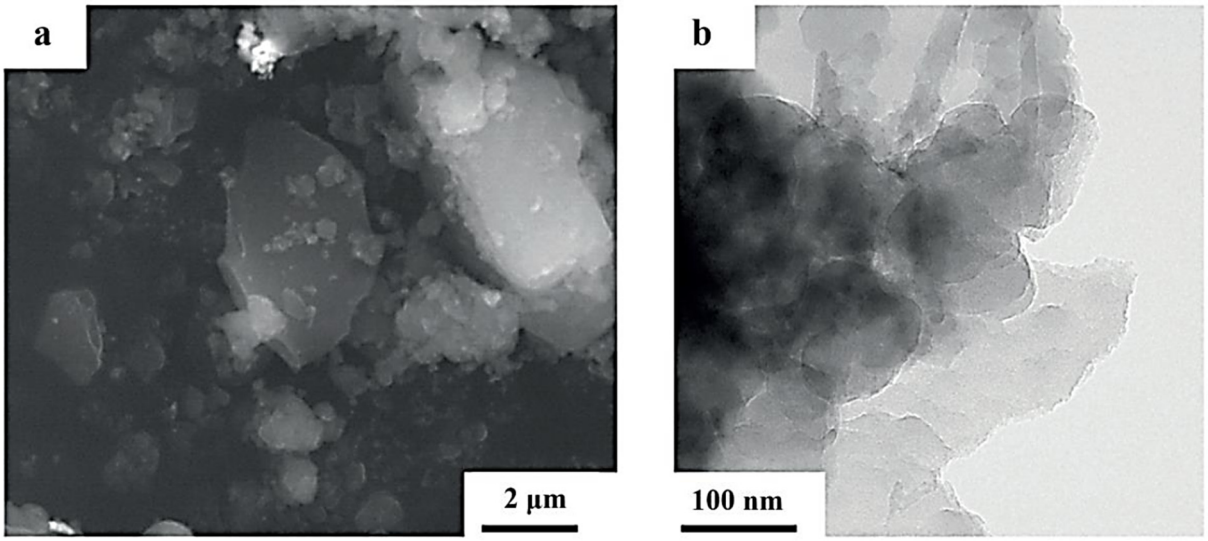

Figure 8. Microphotographs of SEM (**a**) and TEM (**b**) synthesized under the condition of the energy-deficient detonation synthesis of a carbonized product.

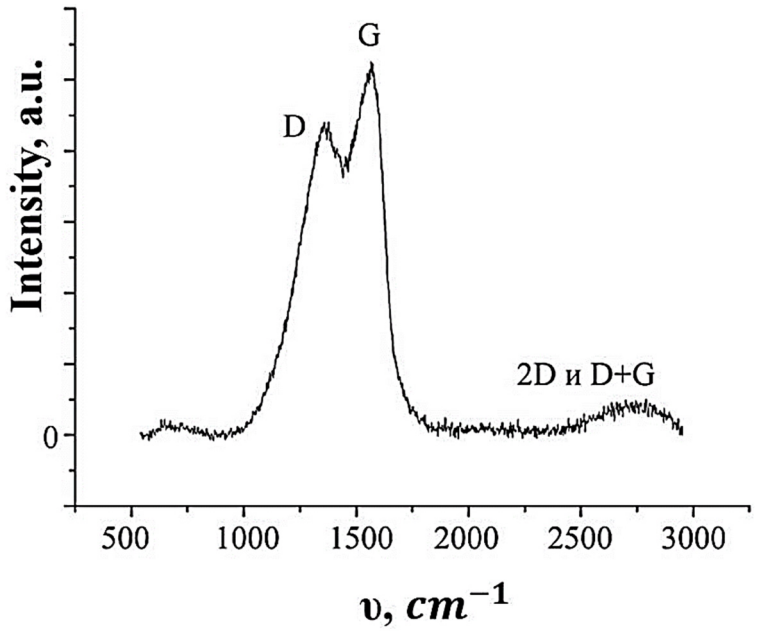

Figure 9. Raman spectrum synthesized under the condition of the energy-deficient detonation synthesis of a carbonized product.

However, we can make some of the following conclusions based on our experimental results. Mechanisms of detonation and SHS syntheses have much in common, and the formation of nanoparticles, in the general case, combines a high-rate formation of initial primitives with their low growth rate.

The formation of nanocarbon particles is determined by the diffusion rate of quantum primitives to the embryo of nanoparticles through their movement over a considerably

considerable distance. The size of a growing particle is proportional to the square root of the particle growth time [11]. The growth of particles is limited by interfacial turbulence resulting from an unequal media density, a gradient of concentrations, and temperatures.

The difference in the mechanisms of the detonation synthesis of 3D nanocarbons (DNDs) and the SHS synthesis of 2D graphene structures, in the most general case, is the result of different amounts of supplied energy.

6. Conclusions

Few-layer graphene, synthesized by natural biopolymer–lignin carbonization under the conditions of the authors' developed process of self-propagating high-temperature synthesis, was used in the design of laser cap detonators. It was demonstrated that the introduction of synthesized few-layer graphene into the design of laser detonators allowed us to significantly reducing the thresholds of the laser initiation of energetic substances. Increasing the sensitivity of composite pyrotechnic compositions modified with few-layer graphene allowed the use of less powerful radiation sources, reducing the requirements for the source of electricity and allowing the creation of more compact and, respectively, safer civilian laser cap detonators. A phenomenological model of organic compound carbonization with the formation of allotropic forms of carbon under the conditions of comparable carbonization mechanisms (SHS and detonation synthesis) was proposed.

Author Contributions: Conceptualization, A.P.V. and M.A.I.; methodology, A.P.V., A.A.V. and M.A.I.; validation, I.V.S. and G.G.S.; investigation, A.P.V., G.G.S. and A.A.V.; resources, A.P.V. and A.A.V.; data curation, A.P.V.; writing—original draft preparation, A.A.V., A.P.V., G.G.S. and M.A.I.; writing—review and editing, A.A.V., A.P.V., I.V.S. and M.A.I.; visualization, A.A.V.; supervision, M.A.I.; project administration, M.A.I.; funding acquisition, A.A.V. and M.A.I. All authors have read and agreed to the published version of the manuscript.

Funding: The work was supported by the Russian Science Foundation grant No. 23-79-10254.

Data Availability Statement: The data presented in this study are available upon reasonable request from the corresponding author.

Conflicts of Interest: The authors declare that there are no conflicts of interest requiring disclosure in this article.

References

1. Lee, P.R. Explosives Development and Fundamentals of Explosives Technology. In *Explosive Effects and Applications. High-Pressure Shock Compression of Condensed Matter*; Zukas, J.A., Walters, W.P., Eds.; Springer: New York, NY, USA, 1998. [CrossRef]
2. Badgujar, D.; Talawar, M.; Asthana, S.; Mahulikar, P. Advances in science and technology of modern energetic materials: An overview. *J. Hazard. Mater.* **2008**, *151*, 289–305. [CrossRef]
3. Ahmad, S.R.; Cartwright, M. *Laser Ignition of Energetic Materials*; John Wiley & Sons: Chichester, UK, 2015; ISBN 9780470975985.
4. *Ecotoxicology of Explosives*; Sunahara, G.I.; Lotufo, G.; Kuperman, R.G.; Hawari, J. (Eds.) Taylor and Francis Group: London, UK; New York, NY, USA, 2009.
5. Fu, X.; Zhu, Y.; Li, J.; Jiang, L.; Zhao, X.; Fan, X. Preparation, Characterization and Application of Nano-Graphene-Based Energetic Materials. *Nanomaterials* **2021**, *11*, 2374. [CrossRef]
6. Liu, Y.; Hu, L.-S.; Gong, S.; Guang, C.; Li, L.; Hu, S.; Deng, P. Study of Ammonium Perchlorate-based Molecular Perovskite $(H_2DABCO)[NH_4(ClO_4)_3]$/Graphene Energetic Composite with Insensitive Performance. *Cent. Eur. J. Energetic Mater.* **2020**, *17*, 451–469. [CrossRef]
7. Cai, W.; Zeng, B.; Liu, J.; Guo, J.; Li, N.; Chen, L.; Chen, H. Improved field emission property of graphene by laser irradiation. *Appl. Surf. Sci.* **2013**, *284*, 113–117. [CrossRef]
8. Zhang, X.; Hikal, W.M.; Zhang, Y.; Bhattacharia, S.K.; Li, L.; Panditrao, S.; Wang, S.; Weeks, B.L. Direct laser initiation and improved thermal stability of nitrocellulose/graphene oxide nanocomposites. *Appl. Phys. Lett.* **2013**, *102*, 141905. [CrossRef]
9. Adel, M.; El-Maghraby, A.; El-Shazly, O.; El-Wahidy, E.-W.F.; Mohamed, M.A.A. Synthesis of few-layer graphene-like nanosheets from glucose: New facile approach for graphene-like nanosheets large-scale production. *J. Mater. Res.* **2016**, *31*, 455–467. [CrossRef]
10. Liu, C.; Li, X.; Li, R.; Yang, Q.; Zhang, H.; Yang, B.; Yang, G. Laser ignited combustion of graphene oxide/nitrocellulose membranes for solid propellant micro thruster and solar water distillation. *Carbon* **2020**, *166*, 138–147. [CrossRef]
11. Voznyakovskii, A.; Neverovskaya, A.; Otvalko, J.; Gorelova, E.; Zabelina, A. Facile synthesis of 2D carbon structures as a filler for polymer composites. *Nanosyst. Phys. Chem. Math.* **2018**, *9*, 125–128. [CrossRef]

12. Sytschev, A.E.; Merzhanov, A.G. Self-propagating high-temperature synthesis of nanomaterials. *Russ. Chem. Rev.* **2004**, *73*, 147–159. [CrossRef]
13. Rogachev, A.S.; Mukasin, A.S. *Combustion for the Synthesis of Materials: An Introduction to Structural Macrokinetics*; physmatlit: Moscow, Russia, 2012.
14. Merzhanov, A. Self-Propagating High-Temperature Synthesis: Non-Equilibrium Processes and Equilibrium Products. *Adv. Sci. Technol.* **2006**, *45*, 36–44.
15. Merzhanov, A.G.; Borovinskaya, I.P. Historical retrospective of SHS: An autoreview. *Int. J. Self Propagating High Temp. Synth.* **2008**, *17*, 242–265. [CrossRef]
16. Mahmoudi, T.; Wang, Y.; Hahn, Y.-B. Graphene and its derivatives for solar cells application. *Nano Energy* **2018**, *47*, 51–65. [CrossRef]
17. Ralph, J.; Lapierre, C.; Boerjan, W. Lignin structure and its engineering. *Curr. Opin. Biotechnol.* **2019**, *56*, 240–249. [CrossRef] [PubMed]
18. Bajwa, D.S.; Pourhashem, G.; Ullah, A.H.; Bajwa, S.G. A concise review of current lignin production, applications, products and their environmental impact. *Ind. Crops Prod.* **2019**, *139*, 111526. [CrossRef]
19. Hardt, A.P. Pyrotechnics. In *Post Falls*; Pyrotechnica Publications: Post Falls, ID, USA, 2001.
20. Zegrya, G.G.; Savenkov, G.G.; Zegrya, A.G.; Bragin, V.A.; Os'kin, I.A.; Poberezhnaya, U.M. Laser Initiation of Energy-Saturated Composites Based on Nanoporous Silicon. *Technol. Phys.* **2020**, *65*, 1636–1642. [CrossRef]
21. Fan, Z.; Wang, K.; Wei, T.; Yan, J.; Song, L.; Shao, B. An environmentally friendly and efficient route for the reduction of graphene oxide by aluminum powder. *Carbon* **2010**, *48*, 1686–1689. [CrossRef]
22. Cheng, I.F.; Xie, Y.; Gonzales, R.A.; Brejna, P.R.; Sundararajan, J.P.; Kengne, B.F.; Aston, D.E.; McIlroy, D.N.; Foutch, J.D.; Griffiths, P.R. Synthesis of graphene paper from pyrolyzed asphalt. *Carbon* **2011**, *49*, 2852–2861. [CrossRef]
23. Panahi-Kalamuei, M.; Amiri, O.; Salavati-Niasari, M. Green hydrothermal synthesis of high quality single and few layers graphene sheets by bread waste as precursor. *J. Mater. Res. Technol.* **2020**, *9*, 2679–2690. [CrossRef]
24. Wang, X.; Liu, Q.; Wu, S.; Xu, B.; Xu, H. Multilayer Polypyrrole Nanosheets with Self-Organized Surface Structures for Flexible and Efficient Solar–Thermal Energy Conversion. *Adv. Mater.* **2019**, *31*, e1807716. [CrossRef]
25. Katsnelson, M.I. *Graphene: Carbon in Two Dimensions*, 2nd ed.; Cambridge University Press: Cambridge, UK, 2012.
26. Ilki, B.; Petrovska, S.; Sergiienko, R.; Tomai, T.; Shibata, E.; Nakamura, T.; Honma, I.; Zaulychnyy, Y. X-Ray Emission Spectra of Graphene Nanosheets. *J. Nanosci. Nanotechnol.* **2012**, *12*, 8913–8919. [CrossRef]
27. Tuz Johra, F.; Lee, J.-W.; Jung, W.-G. Facile and safe graphene preparation on solution based platform. *J. Ind. Eng. Chem.* **2014**, *20*, 2883–2887. [CrossRef]
28. Bezuidenhout, H.C.; Mukhopadhyay, S. Nanoporous Silicon Based Energetic Formulations for Use in Explosives Initiating System. *Int. J. Appl. Eng. Res.* **2016**, *11*, 10465–10471.
29. Zegrya, G.G.; Savenkov, G.G.; Morozov, V.A.; Ulin, N.V.; Ulin, V.P.; Lukin, A.A.; Bragin, V.A.; Oskin, I.A.; Mikhailov, Y.M. Sensitivity of energy-packed compounds based on superfine and nanoporous silicon to pulsed electrical treatments. *Semiconductors* **2017**, *51*, 477–482. [CrossRef]
30. Grobler, J.M.; Focke, W.W.; Tichapondwa, S.M.; Montgomery, Y.C. Pyrotechnic Alternatives to Primary Explosive-Based Initiators. In *Nano and Micro-Scale Energetic Materials: Propellants and Explosives*; Pang, W., DeLuca, L.T., Eds.; Part VI: Primary and Secondary Explosives. Chapter 17; Wiley-VCH: Weinheim, Germany, 2023; Volume 2, pp. 499–540. [CrossRef]
31. Ilyushin, M.A.; Voznyakovskii, A.P.; Shugalei, I.V.; Tverjanovich, A.S. Laser initiation of modified complex cobalt (III) perchlorate. *Z. Für Anorg. Und Allg. Chem.* **2021**, *647*, 1254–1260. [CrossRef]
32. Yan, Q.-L.; Gozin, M.; Zhao, F.-Q.; Cohen, A.; Pang, S.-P. Highly energetic compositions based on functionalized carbon nanomaterials. *Nanoscale* **2016**, *8*, 4799–4851. [CrossRef]
33. Poberezhnaya, U.M.; Freiman, V.M.; Ilyushin, M.A.; Zegrya, G.G.; Fadeev, D.V.; Os'kin, I.A.; Morozov, V.A.; Grigor'ev, A.Y.; Savenkov, G.G. Optical and electron-beam initiation of porous silicon films with different contents of oxidizer and graphene. *Tech. Phys.* **2022**, *67*, 1469–1474. [CrossRef]
34. Balandin, A.A.; Ghosh, S.; Bao, W.; Calizo, I.; Teweldebrhan, D.; Miao, F.; Lau, C.N. Superior Thermal Conductivity of Single-Layer Graphene. *Nano Lett.* **2008**, *8*, 902–907. [CrossRef]
35. Huang, X.; Zhi, C.; Lin, Y.; Bao, H.; Wu, G.; Jiang, P.; Mai, Y.-W. Thermal conductivity of graphene-based polymer nanocomposites. *Mater. Sci. Eng. R Rep.* **2020**, *142*, 100577. [CrossRef]
36. Mbambo, M.C.; Khamlich, S.; Khamliche, T.; Moodley, M.K.; Kaviyarasu, K.; Madiba, I.G.; Madito, M.J.; Khenfouch, M.; Kennedy, J.; Henini, M.; et al. Remarkable thermal conductivity enhancement in Ag—Decorated graphene nanocomposites based nanofluid by laser liquid solid interaction in ethylene glycol. *Sci. Rep.* **2020**, *10*, 10982. [CrossRef]
37. Mbambo, M.C.; Madito, M.J.; Khamliche, T.; Mtshali, C.B.; Khumalo, Z.M.; Madiba, I.G.; Mothudi, B.M.; Maaza, M. Thermal conductivity enhancement in gold decorated graphene nanosheets in ethylene glycol based nanofluid. *Sci. Rep.* **2020**, *10*, 14730. [CrossRef]
38. Volkov, K.V.; Danilenko, V.V.; Elin, V.I. Synthesis of diamond from the carbon in the detonation products of explosives. *Combust. Explos. Shock Waves* **1990**, *26*, 366–368. [CrossRef]
39. Danilenko, V.V. Specific Features of Synthesis of Detonation Nanodiamonds. *Combust. Explos. Shock Waves* **2005**, *41*, 577–588. [CrossRef]

40. Titov, V.M.; Anisichkin, V.F.; Mal'Kov, I.Y. Synthesis of ultradispersed diamond in detonation waves. *Combust. Explos. Shock Waves* **1989**, *25*, 372–379. [CrossRef]
41. Pershin, S.V.; Petrov, E.A.; Tsaplin, D.I. Influence of the molecular structure of explosives on the rate of formation, yield, and properties of ultradisperse diamond. *Combust. Explos. Shock Waves* **1994**, *30*, 235–238. [CrossRef]
42. Semenov, N.N. *On Some Problems of Chemical Kinetics and Reactivity*; Publishing House of the USSR Academy of Sciences: Moscow, Russia, 1958. (In Russian)
43. Voznyakovskii, A.P.; Dolmatov, V.Y.; Shumilov, F.A. The influence of detonation synthesis conditions on surface properties of detonation nanodiamonds. *J. Superhard Mater.* **2014**, *36*, 165–170. [CrossRef]
44. Vereshchagin, A.L. *Detonation Nanodiamonds*; ASTU Publishing House: Barnaul, Russia, 2001. (In Russian)